Early candidate biomarkers found from urine of astrocytoma rat before changes in MRI

Yanying Ni [1], Fanshuang Zhang [1], Manxia An[1], Wei Yin[1] and Youhe Gao[1, 2*]

[1] Department of Pathophysiology, Institute of Basic Medical Sciences, Chinese Academy of Medical Sciences, School of Basic Medicine, Peking Union Medical College, Beijing, China

[2] Department of Biochemistry and Molecular Biology, Beijing Normal University, Gene Engineering and Biotechnology Beijing Key Laboratory, Beijing, China

*Corresponding author: Youhe Gao, Department of Biochemistry and Molecular Biology, Beijing Normal University, Gene Engineering and Biotechnology Beijing Key Laboratory, Beijing, 100875, PR. of China, Tel: 86-10- 58804382; E-mail: gaoyouhe@bnu.edu.cn

Abstract

Astrocytoma is the most common aggressive glioma and its early diagnosis remains difficult. Biomarkers are changes associated with the disease. Urine, which is not regulated by homeostatic mechanisms, accumulates changes and therefore is a better source for biomarker discovery. In this study, C6 cells were injected into Wistar rats brain as astrocytoma model. Urine samples were collected at day 2, day 6, day 10 and day 13 after injection, and the urinary proteomes were analyzed. On the 10th day, lesions appeared in magnetic resonance imaging. On the 13th day, clinical symptoms started. But differential urinary proteins were changed with the development of the astrocytoma, and can provide clues even on the 2nd and 6th day. Twenty-seven differential proteins with human orthologs had been reported to associate with astrocytoma. Thirty-nine proteins were verified in four more rats as candidate biomarkers of astrocytoma using multiple-reaction monitoring. A panel of differential urinary proteins may provide early biomarkers for diagnose of astrocytoma.

Keywords: Urine proteome, Animal model, Biomarker, Astrocytoma

Introduction

Gliomas are the most frequent primary tumors of the central nervous system, accounting for more than 60% of all brain tumors [1]. Among them, glioblastoma (GBM) is the most common aggressive glioma, and the average survival rate remains low [2]. The standard combination of surgery and radiotherapy or chemotherapy can only extend the progression-free survival time for 12–18 months, with a high risk of recurrence [3]. In addition, the incidence of astrocytoma has increased annually by 1–2% in the past years [4]. Therefore, a precise early diagnosis of astrocytoma is crucial for the early determination of appropriate therapeutic strategies.

Changes associated with physiological or pathophysiological processes are the most fundamental characteristic of biomarkers [5]. Urine which is not regulated by homeostatic mechanisms, has the potential to accumulate changes and serve as a better source for disease biomarker discovery [6]. However, urine can be affected by various factors, such as age, diet, and drugs [7, 8]. To minimize these confounding factors, animal models were used to mimic the pathophysiological changes of diseases to search for valuable clues, instead of clinical samples [9].

The rapidly proliferating rat C6 cell line is morphologically similar to GBM when injected into the brain of neonatal rats [10]. The C6 model is closer to the usual histological characteristics of spontaneous GBM when using Wistar rats rather than other strains, including nuclear pleomorphism, high mitotic index, hemorrhage, necrosis and parenchymal invasion [11]. In this study, urine samples were used to identify the candidate biomarkers involved in GBM diagnosis, and further monitor prognosis. The urinary proteome at 2 days, 6 days, 10 days and 13 days was analyzed. This study will not only benefit patients with GBM but also give us a more comprehensive understanding of the clinical significance of urine (Fig.1).

Methods

Ethics statement

All protocols involving animals were approved by the Institute of Basic Medical Sciences Animal Ethics Committee, Peking Union Medical College. Male Wistar rats weighing 200 to 230 g were obtained from the Institute of Laboratory Animal Science, Chinese Academy of Medical Science & Peking Union Medical College. All animals were housed with free access to water and a standard laboratory diet under controlled room temperature (22±1℃) and humidity conditions (65-70%). All efforts were made to minimize suffering.

Cell culture.

Rat C6 cells were obtained from the Chinese Academy of Medical Science & Peking Union Medical College (Beijing, China) and cultured at 37℃ in DMEM, supplemented with 10% fetal bovine serum, 100 IU/mL penicillin and 100 μg/mL streptomycin in a humidified atmosphere of 5% CO2 air (Thermo Fisher Scientific, Inc., Waltham, MA, USA) [12]. Cells in the logarithmic growth phase were used for the experiment.

Rat C6 astrocytoma model.

Male Wistar rats were randomly divided into two groups (20 rats in each group). The astrocytoma model was established as described previously [13]. Briefly, under

general anesthesia with 2% pelltobarbitalum natricum (40 mg/kg body weight), the skull was drilled at 1 mm anterior to the anterior fontanelle and 3 mm right of the midline, and 10 μl of cell suspension containing 106 cells was injected using a microsyringe (SHANGHAI HIGH PIGEON INDUSTRY TRADE & Co., LTD CHINA). Rats in the control group were administrated PBS only. The rats' weights were monitored twice a day. Rats with similar clinical symptom were chosen for further analysis, which will help to find biomarkers in the same period of GBM.

Magnetic resonance imaging analysis

MRI was performed using a 7 T MRI animal system (Agilent, US) on days 6, 10 and 13 after tumor cell implantation. Rats were monitored under anesthesia. The parameters were set as follows: T1 (TR/TE = 500/15.69 ms, 16 slices with FOV $40 \times 40\ mm^2$, matrix = 256 × 256). Acquisition duration was 3 min and 44 s; T2-weighted sequence (TR/TE =3500 ms/72.00 ms, with repetition time 1,000 ms, matrix = 256 × 256) [14].

Brain histopathology

Rats were sacrificed using overdose anesthesia and perfused with 4% paraformaldehyde via the left ventricle. After perfusion with 0.9% saline and ice-cold 4% paraformaldehyde, the brains were removed and post-fixed in 4% paraformaldehyde in PBS overnight, and then the tissues were embedded in paraffin, sliced at 2–3 μm, and stained with hematoxylin and eosin (H&E) [15].

Urinary protein sample preparation and LC-MS/MS analysis

Proteins were extracted as follows [16]: (1) centrifugation at 2000 ×g and 12000 ×g for 30 minutes at 4 ℃, respectively; (2) precipitation by ethanol overnight at 4 ℃; (3) dissolution by lysis buffer (8 M urea, 2 M thiourea, 25 mM dithiothreitol and 50 mM Tris).

For each urine sample, some proteins were separated using sodium dodecyl sulfate polyacrylamide gel electrophoresis (SDS-PAGE), while some proteins were digested by trypsin (Trypsin Gold, Mass Spec Grade, Promega, Fitchburg, WI, USA) in 10-kD filter units (Pall, Port Washington, NY, USA) [17]. UA (8 M urea in 0.1 M Tris-HCl, pH 8.5) was added to wash the proteins at 14000 ×g for 20 min at 18 ℃. NH4HCO3 was added subsequently to wash the protein. Then, the urinary proteins were denatured by dithiothreitol and alkylated by iodoacetamide. The proteins were digested with trypsin at 37 ℃ for 14 hours. The collected peptide mixtures were desalted using Oasis HLB cartridges (Waters, Milford, MA) and then dried by vacuum evaporation (Thermo Fisher Scientific, Bremen, Germany).

The digested peptides were acidified with 0.1% formic acid, then loaded onto a reversed-phase micro-capillary column using a Waters UPLC system. The MS data were acquired using Thermo Orbitrap Fusion Lumos (Thermo Fisher Scientific, Bremen, Germany). Animals (n=3) with the same clinical manifestations were randomly chosen from the astrocytoma group. Each sample was analyzed three times.

Protein identification and label-free quantitation

The MS/MS data were analyzed using Progenesis and Masccot (version 2.4.1, Matrix Science, London, UK). The parameters were set as follows: Swiss-Prot rat database (551,193 sequences; 196,822,649 residues); the fragment tolerance was 0.05 Da; the parent ion tolerance was 0.05 Da; the precursor mass tolerance was 10 ppm; two missed trypsin cleavage sites were allowed; and peptide identifications containing at least 2 identified peptides were accepted, as in a previous study [18]. Carbamidomethylation of cysteines was set as a fixed modification, and oxidation of methionine and protein N-terminal acetylation were set as variable modifications. After normalization, the fold change of abundance was used to analyze differential proteins between the control group and the astrocytoma group [19, 20].

Multiple-Reaction Monitoring analysis

Some differential proteins were validation using multiple-reaction monitoring (MRM). For targeted proteomic analysis, the dat file of GBM urine generated by conventional LC/MS/MS were imported into Skyline version 1.1. software. Skyline was employed to select the most intense peptide transitions, up to four or five transitions per peptide were selected and were traced on a QTRAP 6500 mass spectrometer (AB Sciex, Massachusetts, USA). All MS data were imported into Skyline, which was used for further peptide transitions selection and abundance calculations.

Gene Ontology and Ingenuity Pathway Analysis

All differentially expressed proteins identified between the control and astrocytoma groups were assigned a gene symbol using the Panther database (http://www.pantherdb.org/) and analyzed by Gene Ontology (GO) based on the molecular function, biological processes, and cellular component categories. For biological processes, all differentially expressed proteins were also analyzed by the IPA software (Ingenuity Systems, Mountain View, CA, USA) for pathway analysis, and network analysis.

Statistical analysis

Clinical symptoms , proteome analysis and MRM data were analyzed using the SPSS16.0 software package for statistical analysis. Comparisons between independent

groups were conducted using one-way ANOVA followed by post hoc analysis with the least significant difference (LSD) test or Dunnett′ s T3 test. P-values of less than 0.05 were considered different.

Results and Discussion

Clinical symptoms

After injection with C6 cells, there was no difference in clinical manifestations. However, on the 13th day, some GBM rats showed twitching, tachypnea, drowsiness and low symptom scores. The rats in the control group did not show any symptoms (Fig. 2A). All rats gained weight steadily after tumor cell implantation. Compared with control rats, the GBM rats' weights were significantly lower on the 13th day, and the weight was 1.04-fold higher in the control group than in the GBM group (Fig. 2B).

MRI analysis

Images of rat brains on the 6th day, 10th day and 13th day were obtained. For MRI imaging, the rats were in a supine position. Compared to the left brain, the right brain injected with tumor cells showed no obvious lesion on the 6th day after tumor cell implantation (Fig. 3A). On the 10th day, there was strong enhancement with an obscure boundary in the right brain on the T2 images (Fig. 3B). On the 13th day, the strong enhancement lesions were largger, and the midline shifted on the T2 images, showing an obvious effect of an intracranial placeholder, such as a midline shift (Fig. 3C).

Histopathology

Rats were sacrificed and the brain tissue separated. H&E staining is shown. Compared to normal tissues, there is tumor tissue in the right caudate nucleus on the 13th day (Fig. 4A). The tumor tissue in GBM rats exhibited invasive growth with an ill-defined margin (Fig. 4B). Nuclear condensation, fragmentation and pathologic mitosis are observed in the tumor tissue (Fig. 4C).

Differential urinary proteins

The urinary proteins were analyzed using Thermo Orbitrap Fusion Lumos. The urinary samples of three rats were analyzed three times to provide technical replicates (Table S1). In total, 778 proteins were identified (Table S2), and 124 differential proteins were selected according to the following criteria: 1) proteins with at least two unique peptides were allowed, 2) fold change ≥ 2; and 3) p value < 0.05. All differential proteins were significantly changed in the three rats' urine.

Among the differential proteins, 109 have corresponding human orthologs, out of which 78 were down-regulated more than 2-fold and 31 were up-regulated more than 2-fold (Table 1). Overall, 56 significantly changed proteins were selected in the 2nd day group (D2), 65 proteins in the D6 group, 61 proteins in the D10 group and 27 proteins in the D13 group, respectively. Among them, sixty-five differential proteins were repeatedly identified in different groups (Fig. S1).

On the 2nd and 6th day, GBM rats showed 90 differential urinary proteins with human orthologs. Among all differential proteins, 27 proteins that had been identified in the CSF, blood or brain tissue were reported to be associated with GBM (Table 2).

MRM analysis

Thirty-nine differential proteins, which were changed in all three rats, were selected for further validation in four additional individual urine samples using MRM. To obtain more confidence, 4-5 transitions were used for each peptide (Table S3). For MRM analysis, the technical variation in the triplicate runs was first calculated and 92.58% of proteins with CV < 0.3 (Table S3), indicating that the technical variation of MRM analysis was ideal.

For the differential proteins, 29 were down-regulated more than 2-fold in the MRM validation results. Glutamyl aminopeptidase was down-regulated in D2, D6, D10 and D13 groups, beta-glucuronidase was also significantly decreased in D2, D6 and D10 groups, which were consistent with MS/MS results (Fig 5). And 9 differential proteins were up-regulated more than 2-fold. Neutrophil gelatinase-associated lipocalin (NGAL) showed a significant elevation in D2 group, beta-2-microglobulin was also significantly increased in D13 group, which confirms the results of our proteome analysis. However, the MRM result of some differential proteins, such as growth and differentiation factor-15 (GDF15) and stanniocalcin-1 which had been reported to be associated with GBM, did not showed significant difference between control and D2 group, which may be due to its lower relative abundance, which requires larger samples and deeper identification for validation.

Gene ontology and Ingenuity Pathway Analysis analyses of differential proteins

The differential proteins were analyzed by the PANTHER classification system. In the biological process category (Fig 6A), the percentages of multicellular organismal processes and metabolic processes were overrepresented, whereas the biological adhesion and response to stimulus were underrepresented in astrocytoma group compared with the whole genome data. In the molecular category (Fig 6B), the percentage of catalytic activity was much higher, while the percentages of receptor and signal transducer activity were much lower in the astrocytoma group in relation to

the whole genome data. In the cellular component category (Fig 6C), the membrane was overrepresented in D6/D10 and D13 groups, whereas extracellular region proteins were underrepresented, indicating that the membrane proteins play a role in the pathologic process of astrocytoma.

Canonical signaling pathways were analyzed to better understand the biological features of glioma. Alpha-actinin-4 (ACTN4), which was involved in VEGF signaling, decreased in the urine of three rats, which is consistent with a previous study's finding that ACTN4 plays a role in the development and progression of glioma [21]. The glutathione synthetase, which is involved in glutathione biosynthesis, decreased in urine. VEGF signaling and glutathione biosynthesis were enriched in the D2, D6 and D10 groups, and these results were consistent with previous work [22, 23], indicating that our proteomic data may reflect the information of glioma. In the acute phase response signaling, acute-phase proteins, such as complement C3 and C-reactive protein, which may reflect the inflammation and activation of the innate immune system during the course of glioma [24, 25].

The network analysis showed that the cellular death and survival networks were mostly affected (Fig 6D). Osteopontin (SPP1), which is primarily involved in immune responses, tissue remodeling and biomineralization, is a core component of these networks. NGAL (LCN2), extracellular superoxide dismutase (SOD3) and Beta-2-microglobulin (B2M) were up-regulated in these networks. Complement C3 (C3), Glutathione S-transferase P (GSTP1), alkaline phosphatase (ALPL), lysosomal acid phosphatase (ACP2) and ezrin (EZR) were down-regulated in relation to the control group and have been reported to play roles in GBM [26-28].

Discussion

NGAL complex activity was elevated in brain tumors and somay serve as a molecular marker for brain tumors [29]. NGAL protein may also be involved in glioma drug resistance and clinical prognosis [30]. Ciliary neurotrophic factor receptor subunit alpha, which participates in the formation of tumor-initiating cells in gliomas, is a marker that correlates with histological grade [31]. Serum acute phase reactant proteins were correlated with GBM in relation to their prognosis. Haptoglobin, previously reported to be involved in infection, tumor growth and migration, was identified as a GBM-specific serum marker [32, 33]. Alpha 1-acid glycoprotein, another serum acute phase reactant protein, was also identified in the serum of patient's with GBM [34]. The lysosomal marker cathepsin D (CATD), which was identified on the 6th day, was frequently overexpressed in glioblastomas [35]. The above differential proteins identified during the early stage may help in providing clues for the early diagnosis of the disease.

Some differential proteins were continuously identified in the D2, D6, D10 or D13 groups. Chloride intracellular channel protein 1 expression presented a correlation with glioma, as higher expression levels were observed in tumor tissues [36]. GSTP1 was reported to show higher expression levels in meningeal tumors and GBM [37]. And a significant decrease in aminopeptidase N (AMPN) occurred concomitantly with tumor growth in glioma tissue [38]. These differential proteins continuously identified in the D2, D6, D10 or D13 groups may help in monitoring the development of the disease.

Most of the differentially expressed proteins that had not been reported to be associated with GBM in other studies may also play an important role and serve as new markers during the progression of this disease. For example, secreted phosphoprotein 24, a bone matrix protein that can suppress pancreatic cancer growth [39] and lung cancer [40], may also be potential urinary markers of GBM.

Several differential proteins may appear in many different brain diseases. For example, AMPN was increased in the urine of both GBM rats and obstructive nephropathy rat [41]; CATD was decreased in the urine of GBM rats but increased in the urine of bladder cancer rats [42], which suggests that these diseases may share similar pathological processes [43]. Thus, it may be difficult to provide an accurate diagnosis using a single biomarker; a panel or collection of urinary proteins may be faster and more sensitive [44]. In this study, one hundred and nine differential proteins with human orthologs could be evaluated together to reflect the progression of GBM.

Compared to the urinary biomarker panel of another cancer, ovarian carcinoma, the protein changes in this study were substantially different. Distinct differential proteins were present in GBM and ovarian carcinoma [45]. The expression profile of differentially expressed proteins in different cancers illustrates that specific pathological conditions have their own biomarker combinations, and different diseases can be differentiated using different biomarker combinations.

In summary, clinical manifestation may provide clues to astrocytoma on the 13th day after tumor cell implantation, while the enhancement lesion appeared in MRI on the 10th day. However, the urinary differential proteins of three rats were changed with the development of the disease and can provide valuable clues by the 2nd and 6th day. Among all the differential proteins in the early stage, 18 proteins were reported to be associated with GBM, suggesting that a panel or collection of urinary differential proteins in urine is a better choice for the early diagnosis of brain diseases (Fig 7). In future studies, we hope this work will help to identify astrocytoma biomarkers with clinical utility and will help to understand the role of urine as a better source in biomarker discovery, especially in brain diseases.

Acknowledgements

This work was supported by the National Key Research and Development Program of China (2016 YFC 1306300); the National Basic Research Program of China (2013CB530850); Beijing Natural Science Foundation (7173264, 7172076) and funds from Beijing Normal University (11100704, 10300-310421102).

1. Wang, J.Y., Bettegowda, C.（2015）Genetics and immunotherapy: using the genetic landscape of gliomas to inform management strategies. J Neurooncol 123： 373-83.
2. Chen, L., Li, X., Liu, L., Yu, B., Xue, Y. et al.（2015）Erastin sensitizes glioblastoma cells to temozolomide by restraining xCT and cystathionine-gamma-lyase function. Oncol Rep 33： 1465-74.
3. Li, J.H., Song, D.Y., Xu, Y.G., Huang, Z., Yue, W.（2008）In vitro study of haematoporphyrin monomethyl ether-mediated sonodynamic effects on C6 glioma cells. Neurol Sci 29： 229-35.
4. Louis, D.N., Ohgaki, H., Wiestler, O.D., Cavenee, W.K., Burger, P.C. et al.（2007）The 2007 WHO classification of tumours of the central nervous system. Acta Neuropathol 114： 97-109.
5. Gao, Y.（2014）Roadmap to the Urine Biomarker Era. MOJ Proteomics & Bioinformatics 1： 00005.
6. Gao, Y.（2013）Urine-an untapped goldmine for biomarker discovery? Sci China Life Sci 56： 1145-6.
7. Mullen, W., Gonzalez, J., Siwy, J., Franke, J., Sattar, N. et al.（2011）A pilot study on the effect of short-term consumption of a polyphenol rich drink on biomarkers of coronary artery disease defined by urinary proteomics. J Agric Food Chem 59： 12850-7.
8. Wu, J., Gao, Y.（2015）Physiological conditions can be reflected in human urine proteome and metabolome. Expert Rev Proteomics 12： 623-36.
9. Kinross, J.M., Drymousis, P., Jimenez, B., Frilling, A.（2013）Metabonomic profiling: a novel approach in neuroendocrine neoplasias. Surgery 154： 1185-92; discussion 1192-3.
10. Auer, R.N., Del Maestro, R.F., Anderson, R.（1981）A simple and reproducible experimental in vivo glioma model. Can J Neurol Sci 8： 325-31.
11. San-Galli, F., Vrignaud, P., Robert, J., Coindre, J.M., Cohadon, F.（1989）Assessment of the experimental model of transplanted C6 glioblastoma in Wistar rats. J Neurooncol 7： 299-304.
12. Pinheiro, A.M., Costa, S.L., Freire, S.M., Almeida, M.A., Tardy, M. et al.（2006）Astroglial cells in primary culture: a valid model to study Neospora caninum infection in the CNS. Vet Immunol Immunopathol 113： 243-7.
13. Zelenkov, P., Baumgartner, R., Bise, K., Heide, M., Meier, R. et al.（2007）Acute morphological sequelae of photodynamic therapy with 5-aminolevulinic acid in the C6 spheroid model. J Neurooncol 82： 49-60.
14. Ulmer, S., Reeh, M., Krause, J., Herdegen, T., Heldt-Feindt, J. et al.（2008）Dynamic contrast-enhanced susceptibility-weighted perfusion MRI (DSC-MRI) in a glioma model of the rat brain using a conventional receive-only surface coil with a inner diameter of 47 mm at a clinical 1.5 T scanner. J Neurosci Methods 172： 168-72.
15. Boretius, S., Escher, A., Dallenga, T., Wrzos, C., Tammer, R. et al.（2012）Assessment of lesion pathology in a new animal model of MS by multiparametric MRI and DTI. Neuroimage 59： 2678-88.

16. Sun, W., Li, F., Wu, S., Wang, X., Zheng, D. et al.（2005）Human urine proteome analysis by three separation approaches. Proteomics 5： 4994-5001.
17. Wisniewski, J.R., Zougman, A., Nagaraj, N., Mann, M.（2009）Universal sample preparation method for proteome analysis. Nat Methods 6： 359-62.
18. Yuan, Y., Zhang, F., Wu, J., Shao, C., Gao, Y.（2015）Urinary candidate biomarker discovery in a rat unilateral ureteral obstruction model. Sci Rep 5： 9314.
19. Schmidt, C., Gronborg, M., Deckert, J., Bessonov, S., Conrad, T. et al.（2014）Mass spectrometry-based relative quantification of proteins in precatalytic and catalytically active spliceosomes by metabolic labeling (SILAC), chemical labeling (iTRAQ), and label-free spectral count. Rna 20： 406-20.
20. Old, W.M., Meyer-Arendt, K., Aveline-Wolf, L., Pierce, K.G., Mendoza, A. et al.（2005）Comparison of label-free methods for quantifying human proteins by shotgun proteomics. Mol Cell Proteomics 4： 1487-502.
21. Quick, Q., Skalli, O.（2010）Alpha-actinin 1 and alpha-actinin 4: contrasting roles in the survival, motility, and RhoA signaling of astrocytoma cells. Exp Cell Res 316： 1137-47.
22. Ren, T., Lin, S., Wang, Z., Shang, A.（2016）Differential proteomics analysis of low- and high-grade of astrocytoma using iTRAQ quantification. Onco Targets Ther 9： 5883-5895.
23. Szeliga, M., Albrecht, J.（2016）Glutamine Metabolism in Gliomas. Adv Neurobiol 13： 259-273.
24. Nijaguna, M.B., Schroder, C., Patil, V., Shwetha, S.D., Hegde, A.S. et al.（2015）Definition of a serum marker panel for glioblastoma discrimination and identification of Interleukin 1beta in the microglial secretome as a novel mediator of endothelial cell survival induced by C-reactive protein. J Proteomics 128： 251-61.
25. Cheng, Y.X., Li, F., Lu, J.Y., Li, M., Du, P. et al.（2011）Growth of G422 glioma implanted in the mouse brain was affected by the immune ability of the host. Chin Med J (Engl) 124： 1994-8.
26. Iwadate, Y., Matsutani, T., Hirono, S., Shinozaki, N., Saeki, N.（2016）Transforming growth factor-beta and stem cell markers are highly expressed around necrotic areas in glioblastoma. J Neurooncol 129： 101-7.
27. Tynninen, O., Carpen, O., Jaaskelainen, J., Paavonen, T., Paetau, A.（2004）Ezrin expression in tissue microarray of primary and recurrent gliomas. Neuropathol Appl Neurobiol 30： 472-7.
28. Kijewska, M., Kocyk, M., Kloss, M., Stepniak, K., Korwek, Z. et al.（2016）The embryonic type of SPP1 transcriptional regulation is re-activated in glioblastoma. Oncotarget
29. Liu, M.F., Hu, Y.Y., Jin, T., Xu, K., Wang, S.H. et al.（2015）Matrix Metalloproteinase-9/Neutrophil Gelatinase-Associated Lipocalin Complex Activity in Human Glioma Samples Predicts Tumor Presence and Clinical Prognosis. Dis Markers 2015： 138974.
30. Zheng, L.T., Lee, S., Yin, G.N., Mori, K., Suk, K.（2009）Down-regulation of lipocalin 2 contributes to chemoresistance in glioblastoma cells. J Neurochem 111： 1238-51.
31. Lu, J., Ksendzovsky, A., Yang, C., Mehta, G.U., Yong, R.L. et al.（2012）CNTF receptor subunit alpha as a marker for glioma tumor-initiating cells and tumor grade: laboratory investigation. J Neurosurg 117： 1022-31.
32. Kumar, D.M., Thota, B., Shinde, S.V., Prasanna, K.V., Hegde, A.S. et al.（2010）Proteomic identification of haptoglobin alpha2 as a glioblastoma serum biomarker: implications in cancer cell migration and tumor growth. J Proteome Res 9： 5557-67.
33. Gollapalli, K., Ray, S., Srivastava, R., Renu, D., Singh, P. et al.（2012）Investigation of serum

proteome alterations in human glioblastoma multiforme. Proteomics 12： 2378-90.

34. Matsuura, H., Nakazawa, S.（1985）Prognostic significance of serum alpha 1-acid glycoprotein in patients with glioblastoma multiforme: a preliminary communication. J Neurol Neurosurg Psychiatry 48： 835-7.
35. Giatromanolaki, A., Sivridis, E., Mitrakas, A., Kalamida, D., Zois, C.E. et al.（2014）Autophagy and lysosomal related protein expression patterns in human glioblastoma. Cancer Biol Ther 15： 1468-78.
36. Setti, M., Osti, D., Richichi, C., Ortensi, B., Del Bene, M. et al.（2015）Extracellular vesicle-mediated transfer of CLIC1 protein is a novel mechanism for the regulation of glioblastoma growth. Oncotarget 6： 31413-27.
37. Stavrinou, P., Mavrogiorgou, M.C., Polyzoidis, K., Kreft-Kerekes, V., Timmer, M. et al.（2015）Expression Profile of Genes Related to Drug Metabolism in Human Brain Tumors. PLoS One 10： e0143285.
38. Ramirez-Exposito, M.J., Mayas-Torres, M.D., Carrera-Gonzalez, M.P., Jimenez-Pulido, S.B., Illan-Cabeza, N.A. et al.（2014）Silver(I)/6-hydroxyiminolumazine compounds differently modify renin-angiotensin system-regulating aminopeptidases A and N in human neuroblastoma and glioma cells. J Inorg Biochem 138： 56-63.
39. Li, C.S., Tian, H., Zou, M., Zhao, K.W., Li, Y. et al.（2015）Secreted phosphoprotein 24 kD (Spp24) inhibits growth of human pancreatic cancer cells caused by BMP-2. Biochem Biophys Res Commun 466： 167-72.
40. Lee, K.B., Murray, S.S., Duarte, M.E., Spitz, J.F., Johnson, J.S. et al.（2011）Effects of the bone morphogenetic protein binding protein spp24 (secreted phosphoprotein 24 kD) on the growth of human lung cancer cells. J Orthop Res 29： 1712-8.
41. Schaffer, P., Molnar, L., Lukasz, P., Mattyus, I., Verebely, T. et al.（2002）[Urinary enzyme excretion in childhood uropathy]. Orv Hetil 143： 2135-9.
42. Osman, I., Bajorin, D.F., Sun, T.T., Zhong, H., Douglas, D. et al.（2006）Novel blood biomarkers of human urinary bladder cancer. Clin Cancer Res 12： 3374-80.
43. Shao, C., Li, M., Li, X., Wei, L., Zhu, L. et al.（2011）A tool for biomarker discovery in the urinary proteome: a manually curated human and animal urine protein biomarker database. Mol Cell Proteomics 10： M111.010975.
44. Zhao, M., Li, M., Li, X., Shao, C., Yin, J. et al.（2014）Dynamic changes of urinary proteins in a focal segmental glomerulosclerosis rat model. Proteome Sci 12： 42.
45. Abdullah-Soheimi, S.S., Lim, B.K., Hashim, O.H., Shuib, A.S.（2010）Patients with ovarian carcinoma excrete different altered levels of urine CD59, kininogen-1 and fragments of inter-alpha-trypsin inhibitor heavy chain H4 and albumin. Proteome Sci 8： 58.
46. Codo, P., Weller, M., Kaulich, K., Schraivogel, D., Silginer, M. et al.（2016）Control of glioma cell migration and invasiveness by GDF-15. Oncotarget 7： 7732-46.
47. Liu, M.F., Jin, T., Shen, J.H., Shen, Z.Y., Zheng, Z.C. et al.（2011）NGAL and NGALR are frequently overexpressed in human gliomas and are associated with clinical prognosis. J Neurooncol 104： 119-27.
48. Su, J., Guo, B., Zhang, T., Wang, K., Li, X. et al.（2015）Stanniocalcin-1, a new biomarker of glioma progression, is associated with prognosis of patients. Tumour Biol 36： 6333-9.
49. Manjula, S., Aroor, A.R., Raja, A., Rao, S.N., Rao, A.（1992）Elevation of serum ceruloplasmin levels in brain tumours. Acta Neurol Scand 86： 156-8.

50. Sytinskii, I.A., Chaika, T.V., Blagova, O.E., Konovalova, N.N., Mikhailova, G.N.（1979）[Aminotransferase and dehydrogenase activity in human brain tumours]. Ukr Biokhim Zh (1978) 51： 111-6.
51. Lin, J.P., Pan, B.C., Li, B., Li, Y., Tian, X.Y. et al.（2014）DJ-1 is activated in medulloblastoma and is associated with cell proliferation and differentiation. World J Surg Oncol 12： 373.
52. Martelli, C., Iavarone, F., D'Angelo, L., Arba, M., Vincenzoni, F. et al.（2015）Integrated proteomic platforms for the comparative characterization of medulloblastoma and pilocytic astrocytoma pediatric brain tumors: a preliminary study. Mol Biosyst 11： 1668-83.
53. Ohtaki, S., Wanibuchi, M., Kataoka-Sasaki, Y., Sasaki, M., Oka, S. et al.（2017）ACTC1 as an invasion and prognosis marker in glioma. J Neurosurg 126： 467-475.
54. Yan, H., Yang, K., Xiao, H., Zou, Y.J., Zhang, W.B. et al.（2012）Over-expression of cofilin-1 and phosphoglycerate kinase 1 in astrocytomas involved in pathogenesis of radioresistance. CNS Neurosci Ther 18： 729-36.
55. Wu, H., Yang, L., Liao, D., Chen, Y., Wang, W. et al.（2013）Podocalyxin regulates astrocytoma cell invasion and survival against temozolomide. Exp Ther Med 5： 1025-1029.
56. El Hindy, N., Rump, K., Lambertz, N., Zhu, Y., Frey, U.H. et al.（2013）The functional Aquaporin 1 -783G/C-polymorphism is associated with survival in patients with glioblastoma multiforme. J Surg Oncol 108： 492-8.
57. He, Q., Shi, X., Zhang, L., Yi, C., Zhang, X. et al.（2016）De Novo Glutamine Synthesis: Importance for the Proliferation of Glioma Cells and Potentials for Its Detection With 13N-Ammonia. Mol Imaging 15：
58. Reynes, G., Vila, V., Martin, M., Parada, A., Fleitas, T. et al.（2011）Circulating markers of angiogenesis, inflammation, and coagulation in patients with glioblastoma. J Neurooncol 102： 35-41.
59. Nygren, C., von Holst, H., Mansson, J.E., Fredman, P.（1997）Increased activity of lysosomal glycohydrolases in glioma tissue and surrounding areas from human brain. Acta Neurochir (Wien) 139： 146-50.
60. Han, S., Lv, X., Wang, Y., Gong, H., Zhang, C. et al.（2015）Effect and mechanism of peroxisome proliferator-activated receptor-gamma on the drug resistance of the U-87 MG/CDDP human malignant glioma cell line. Mol Med Rep 12： 2239-46.
61. Kandil, S., Brennan, L., McBean, G.J.（2010）Glutathione depletion causes a JNK and p38MAPK-mediated increase in expression of cystathionine-gamma-lyase and upregulation of the transsulfuration pathway in C6 glioma cells. Neurochem Int 56： 611-9.
62. Bensalma, S., Chadeneau, C., Legigan, T., Renoux, B., Gaillard, A. et al.（2015）Evaluation of cytotoxic properties of a cyclopamine glucuronide prodrug in rat glioblastoma cells and tumors. J Mol Neurosci 55： 51-61.
63. Monod, L., Hamou, M.F., Ronco, P., Verroust, P., de Tribolet, N.（1992）Expression of cALLa/NEP on gliomas: a possible marker of malignancy. Acta Neurochir (Wien) 114： 3-7.

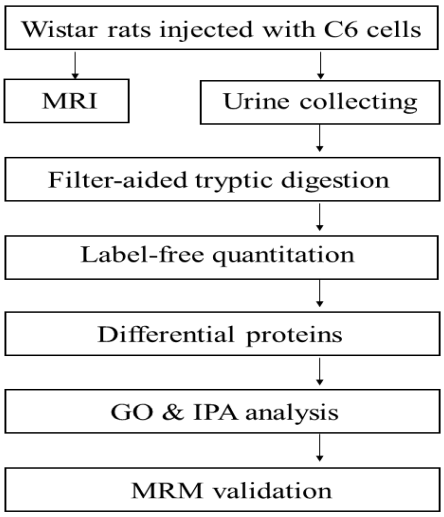

Fig 1. Workflow of protein identification in the GBM rats model. Urine samples were collected from the control and GBM groups. The proteins were analyzed by label-free proteomic analysis. The differential proteins were analyzed by GO and IPA. MRM was used to validate the key differentially expressed proteins.

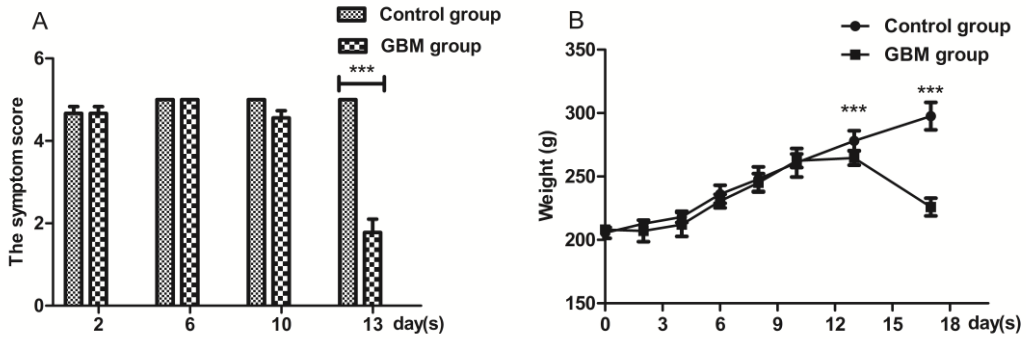

Fig 2. Clinical parameters of rats in control and GBM rats. (a) The symptom scores of GBM rats were significantly decreased on 13th day after tumor cells injection (P=0.001). (b) The weight of GBM rats were significantly decreased on 17th day (P<0.001).

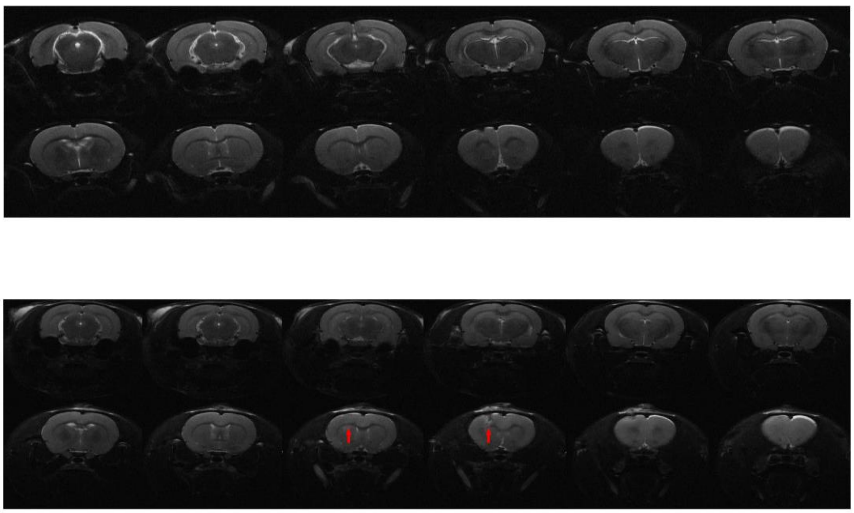

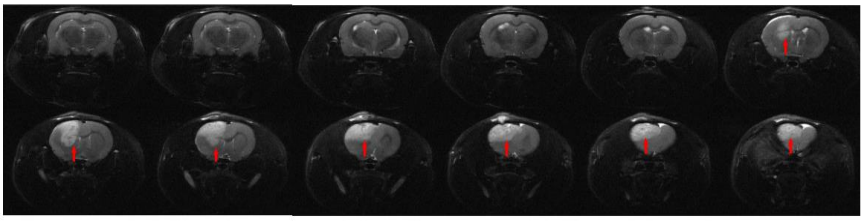

Fig 3. MRI results of the brain tissues after an injection with tumor cells (A) MRI results of the brain tissues on the 6th day. (B) MRI results of the brain tissues on the 10th day. The red arrow indicates the cancer tissues. (C) MRI results of the brain tissues on the 13th day. Red arrows indicate the cancer tissues and the shifted midline.

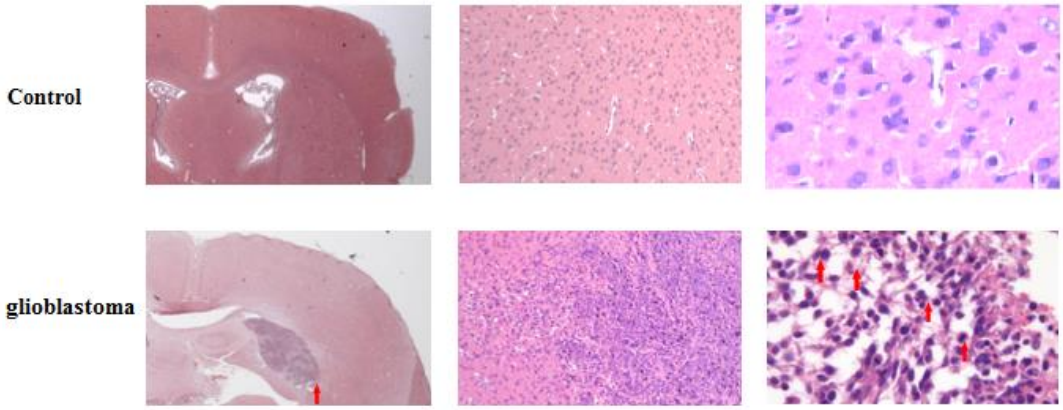

Fig 4. H&E staining of brain tissues on the 13th day after an injection with rat glioma C6 cells. (A) H&E staining (7.5×). The red arrow indicates cancer tissues. (B) H&E staining (100×). (C) H&E staining (400×). The red arrow indicates tumor mitotic figure.

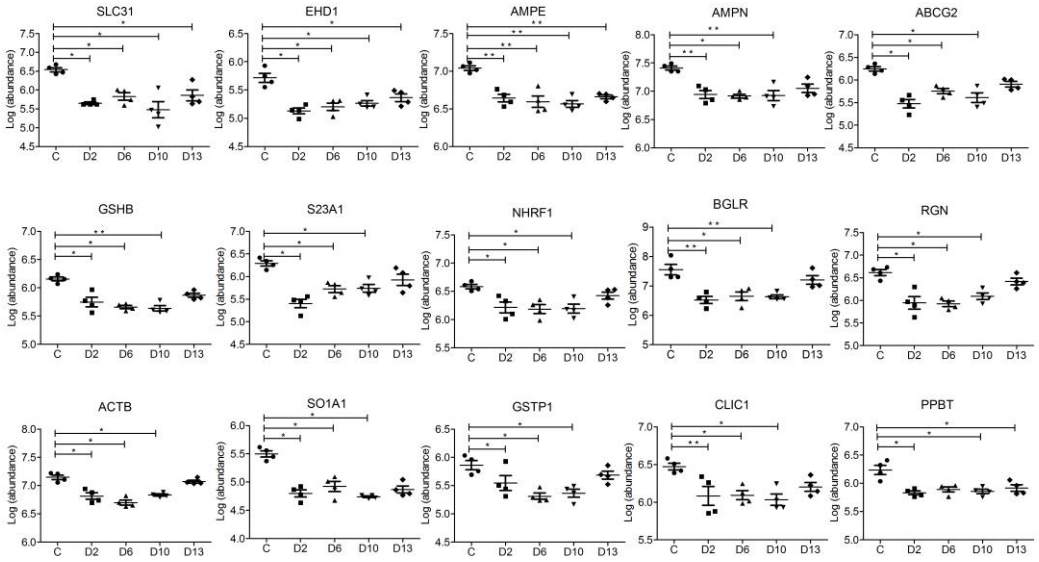

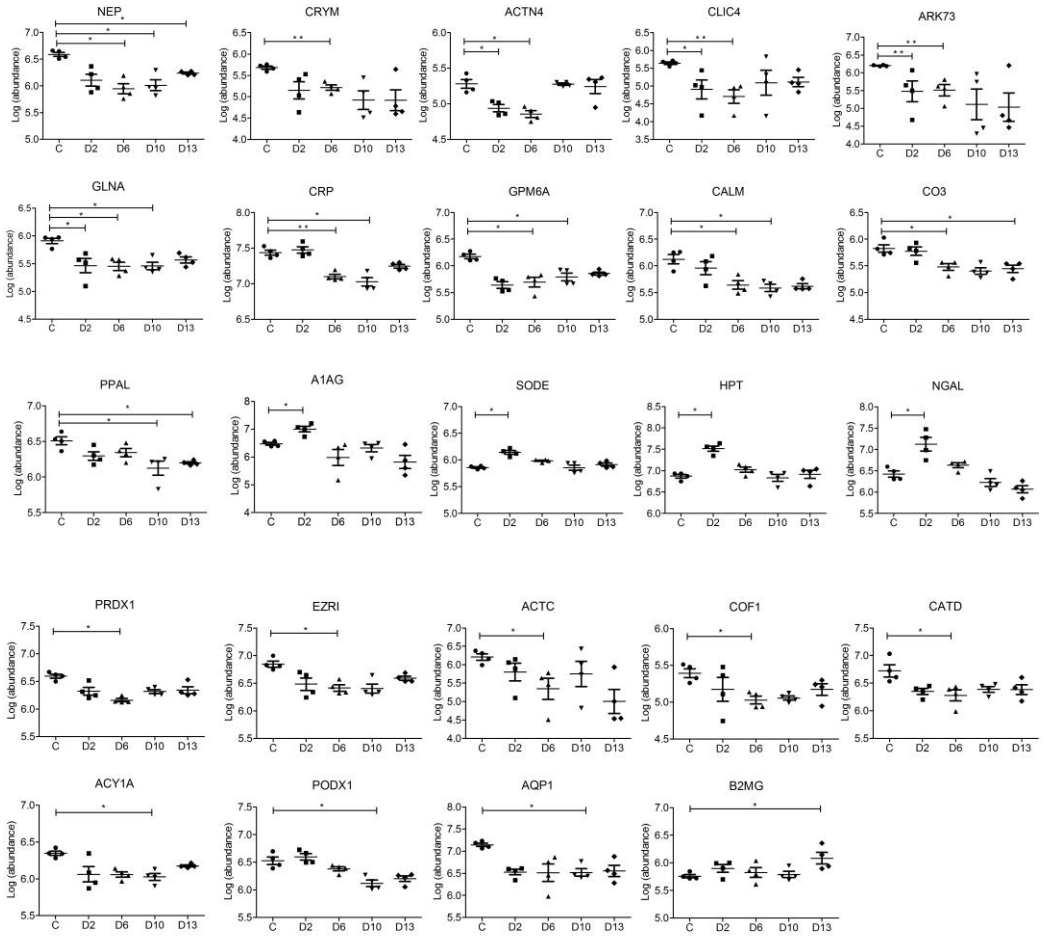

Fig 5. MRM results of candidate urine biomarkers of GBM. Thirty-four proteins shared a decreasing trend in relative abundance, five proteins shared an increasing trend. The x-axis represents different groups; the y-axis refers to the log transformation of the normalized abundance identified by skyline software.

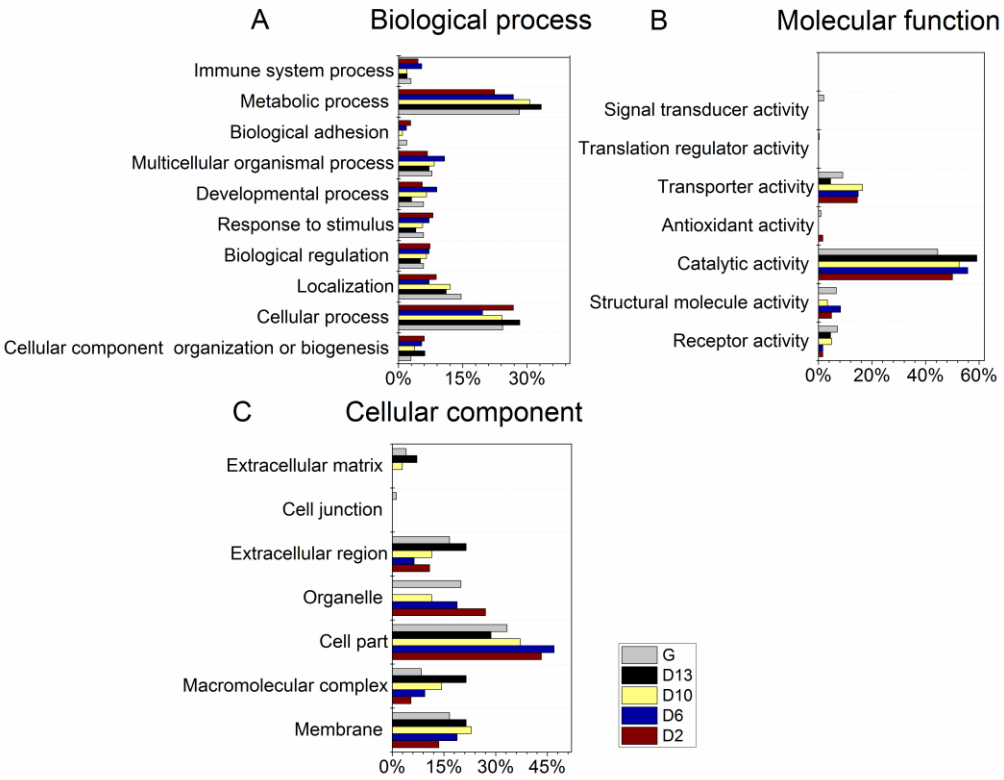

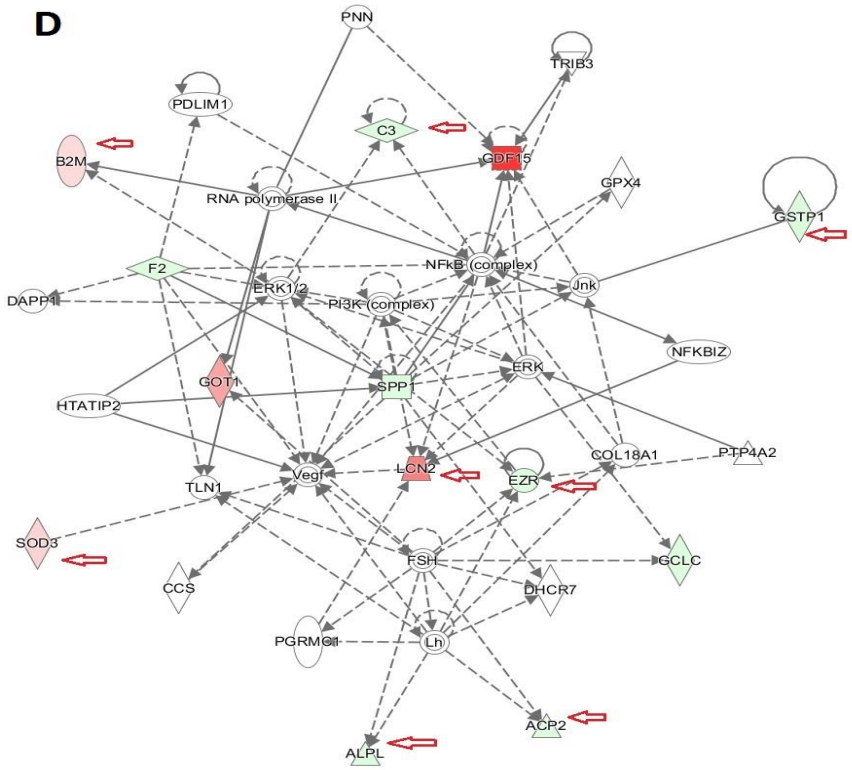

Fig 6. Panther and IPA network analysis of differential proteins. (A) The molecular function analysis between the control and GBM groups; (B) The biological process analysis between the

control and GBM groups. (C) The cellular component analysis between the control and GBM groups.(D) Death and Survival networks from IPA analysis. Proteins in red were up-regulated in GBM compared with control rats, and proteins in green were down-regulated in GBM. Proteins pointed by the red arrow were validated using MRM.

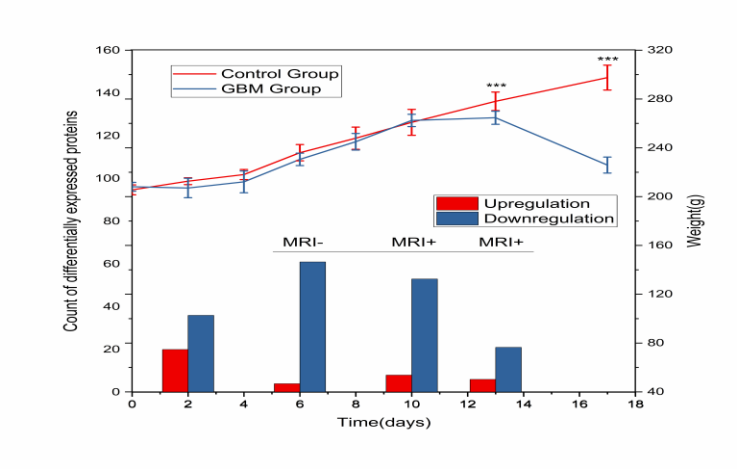

Fig 7. A panel or collection of differential urinary proteins can provide clues for the early diagnose of GBM. Clinical manifestation may provide clues on the 13th day after tumor cell implantation, while the enhancement lesion appeared in MRI on the 10th day. However, the urinary differential proteins of three rats can provide valuable clues by the 2nd and 6th day.

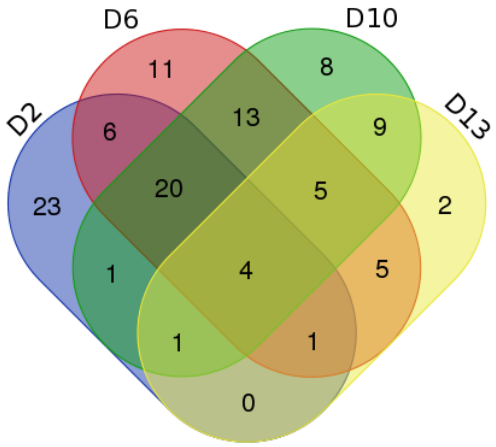

Fig S1. The differential proteins identified in GBM rats. Compared with control group, four proteins were identified in all four GBM groups; twenty-seven proteins were identified in three GBM groups; thirty-four proteins were identified in two GBM groups.

Table 1. Number of up-regulated and down-regulated differential proteins in different GBM groups.

Group	Upregulation	Downregulation	Total
D2	20	36	778
Percentage	2.57	4.62	100
D6	4	61	778
Percentage	0.51	7.84	100
D10	8	53	778

Percentage	1.02	6.81	100
D13	6	21	778
Percentage	0.77	2.69	100
Total (differential proteins)	31	78	109

Table 2. Details of urinary differential proteins identified on the 2nd and 6th day groups.

Uniprot ID	Protein name	Accession	Trend	Fold Change				Associate with GBM	MRM	Candidate biomarker
				D2	D6	D10	D13			
P07911	Uromodulin	UROM	↑	6.37	-	-	-	No	No	Yes
Q99988	Growth/differentiation factor 15	GDF15	↑	12.1	-	-	-	Blood, CSF [46]	No	No
P80188	Neutrophil gelatinase-associated lipocalin	LNC2	↑	7.64	-	-	-	Tissue [47]	Yes	Yes
P52823	Stanniocalcin-1	STC1	↑	3.41	-	-	-	Tissue [48]	No	No
P08294	Extracellular superoxide dismutase [Cu-Zn]	SODE	↑	2.60	-	-	-	No	Yes	Yes
P00739	Haptoglobin	HPT	↑	4.58	-	-	-	Blood [32]	Yes	No
P02763	Alpha-1-acid glycoprotein	A1AG	↑	7.33	-	-	-	Blood [34]	Yes	Yes
P08571	Ceruloplasmin	CERU	↑	2.21	-	-	-	Blood [49]	No	Yes
P07108	Acyl-CoA-binding protein	ACBP	↑	3.43	-	-	-	No	No	Yes
Q13103	Secreted phosphoprotein 24	SPP24	↑	2.80	-	-	-	No	No	No
Q02818	Nucleobindin-1	NUCB1	↑	2.07	-	-	-	No	No	No
P24855	Deoxyribonuclease-1	DNAS1	↑	2.27	-	-	-	No	No	No
Q06033	Inter-alpha-trypsin inhibitor heavy chain H3	ITIH3	↓	0.37	-	-	-	No	No	No
P17174	Aspartate aminotransferase	AATC	↑	5.43	-	-	-	Tissue [50]	No	No
Q99497	Protein deglycase DJ-1	PARK7	↑	3.70	-	-	-	Tumor cells [51]	No	No
P68871	Hemoglobin subunit beta-2	HBB2	↑	8.35	-	-	-	No	No	Yes
P01011	Serine protease inhibitor A3M (Fragment)	SPA3M	↑	2.75	-	-	-	No	No	Yes
P68871	Hemoglobin subunit beta-1	HBB1	↑	13.8	-	-	-	No	No	Yes
P26992	Ciliary neurotrophic factor receptor subunit alpha	CNTFR	↑	2.39	-	-	-	Tissue [31]	No	No
Q99519	Sialidase-1	NEUR1	↓	0.46	-	-	-	No	No	No

O95968	Prostatic steroid-binding protein C1	PSC1	↑	7.75	-	-	-	No	No	No
P02533	Keratin, type I cytoskeletal 14	K1C14	↓	0.25	-	-	-	No	No	No
P55259	Pancreatic secretory granule membrane major glycoprotein GP2	GP2	↑	4.98	-	-	-	No	No	No
Q06830	Peroxiredoxin-1	PRDX1	↓	-	0.34	-	-	Tissue [52]	Yes	No
P52758	Ribonuclease UK114	UK114	↓	-	0.49	-	-	No	No	No
P02768	Serum albumin	ALBU	↓	-	0.48	-	-	No	No	Yes
P68032	Actin, alpha cardiac muscle 1	ACTC	↓	-	0.46	-	-	Tissue [53]	Yes	No
P07339	Cathepsin D	CATD	↓	-	0.47	-	-	Tumor cells [35]	Yes	No
P15311	Ezrin	EZRI	↓	-	0.46	-	-	Tissue [27]	Yes	No
P68104	Elongation factor 1-alpha 1	EF1A1	↓	-	0.34	-	-	No	No	No
P0CG47	Polyubiquitin-B	UBB	↓	-	0.43	-	-	No	No	No
Q96BW5	Phosphotriesterase-related protein	PTER	↓	-	0.42	-	-	No	No	No
P23528	Cofilin-1	COF1	↓	-	0.40	-	-	Tissue [54]	Yes	No
P01834	Ig kappa chain C region, A allele	KACA	↑	-	3.13	-	-	No	No	Yes
O00592	Podocalyxin	PODXL	↓			0.47		Yes [55]	Yes	Yes
P21281	V-type proton ATPase subunit B, brain isoform	VATB2	↓			0.45		No	No	No
P00995	Serine protease inhibitor Kazal-type 1-like	ISK1L	↓			0.32		No	No	Yes
P49189	4-trimethylaminobutyraldehyde dehydrogenase	AL9A1	↓			0.31		No	No	No
P29972	Aquaporin-1	AQP1	↓			0.49		Yes [56]	Yes	Yes
P06870	Prostatic glandular kallikrein-6	KLK6	↑			2.65		No	No	No
P08118	Beta-microseminoprotein	MSMB	↑			5.87		No	No	Yes
P06870	Submandibular glandular kallikrein-9	KLK9	↑			3.47		No	No	No
P61769	Beta-2-microglobulin	B2MG	↑				2.15	No	Yes	Yes
P07195	L-lactate dehydrogenase B chain	LDHB	↓				0.34	No	No	Yes
Q9HBJ8	Collectrin	TMM27	↓	0.34	0.26	-	-	No	No	No
P15104	Glutamine synthetase	GLNA	↓	0.47	0.42	-	-	Tumor cells [57]	Yes	No
Q92859	Neogenin (Fragment)	NEO1	↓	0.35	0.27	-	-	No	No	No

Q14894	Ketimine reductase mu-crystallin	CRYM	↓	0.44	0.46	-	-	No	Yes	No
O95154	Aflatoxin B1 aldehyde reductase member 3	ARK73	↓	0.25	0.27	-	-	No	Yes	No
O43707	Alpha-actinin-4	ACTN4	↓	0.04	0.15	-	-	Tissue [21]	Yes	No
O14556	Glyceraldehyde-3-phosphate dehydrogenase	G3PT	↓	0.07	-	0.17	-	No	No	No
Q96HD9	N-acyl-aromatic-L-amino acid amidohydrolase	ACY3	↓	-	0.26	0.38	-	No	No	No
Q96KP4	Cytosolic non-specific dipeptidase	CNDP2	↓	-	0.42	0.43	-	No	No	No
P02741	C-reactive protein	CRP	↓	-	0.39	0.42	-	Blood [24]	Yes	Yes
P50053	Ketohexokinase	KHK	↓	-	0.27	0.38	-	No	No	No
Q9H0W9	Ester hydrolase C11orf54 homolog	CK054	↓	-	0.41	0.48	-	No	No	No
P09467	Fructose-1,6-bisphosphatase 1	F16P1;F16P2	↓	-	0.38	0.41	-	No	No	No
Q2TAA2	Isoamyl acetate-hydrolyzing esterase 1 homolog	IAH1	↓	-	0.35	0.42	-	No	No	No
Q86X76	Nitrilase homolog 1	NIT1	↓	-	0.26	0.40	-	No	No	No
Q16820	Meprin A subunit beta	MEP1B	↓	-	0.38	0.46	-	No	No	No
P62158	Calmodulin	CALM	↓	-	0.42	0.49	-	No	Yes	No
P51674	Neuronal membrane glycoprotein M6-a	GPM6A	↓	-	0.27	0.40	-	No	Yes	No
P60174	Triosephosphate isomerase	TPIS	↓	-	0.43	0.47	-	Tissue [52]	No	Yes
Q96DA0	Prostatic spermine-binding protein	SPBP	↑	-	2.78	4.21	-	No	No	No
P01859	Ig gamma-1 chain C region	IGHG1	↑			6.42	9.42	No	No	Yes
P00734	Prothrombin	THRB	↓			0.45	0.43	Yes [58]	No	No
P16112	Aggrecan core protein	PGCA	↓			0.45	0.46	No	No	No
P11117	Lysosomal acid phosphatase	PPAL	↓			0.44	0.48	Yes [59]	Yes	No
P20472	Parvalbumin alpha	PRVA	↑			4.11	3.86	No	No	No
P36896	Activin receptor type-1B	ACV1B	↓			0.48	0.44	No	No	No
P00966	Argininosuccinate synthase	ASSY	↓			0.45	0.41	No	No	No
P10451	Osteopontin	SPP1	↓			0.25	0.29	Yes [28]	No	Yes
P01859	Ig gamma-2A chain C region	IGG2A	↑			2.78	0.45	No	No	No

P01024	Complement C3	CO3	↓	-	0.40	-	0.45	Tissue [25]	Yes	No
O00764	Pyridoxal kinase	PDXK	↓	-	0.19	-	0.21	No	No	No
P01834	Ig kappa chain C region, B allele	KACB	↑	-	2.01	-	2.22	No	No	Yes
Q06495	Sodium-dependent phosphate transport protein 2A	NPT2A	↓	-	0.10	-	0.20	No	No	No
P68371	Tubulin beta-4B chain	TBB4B	↓	-	0.36	-	0.34	No	No	No
P15144	Aminopeptidase N	AMPN	↓	0.33	0.30	0.46	-	Tissue [38]	Yes	No
P48637	Glutathione synthetase	GSHB	↓	0.44	0.20	0.31	-	Tumor cells [60]	Yes	No
Q15493	Regucalcin	RGN	↓	0.28	0.18	0.33	-	No	Yes	No
P19440	Gamma-glutamyltranspeptidase 1	GGT1	↓	0.38	0.31	0.45	-	No	No	Yes
P46721	Solute carrier organic anion transporter family member 1A1	SO1A1	↓	0.07	0.08	0.23	-	No	Yes	No
P48507	Glutamate--cysteine ligase regulatory subunit	GSH0	↓	0.32	0.28	0.40	-	No	No	No
P32929	Cystathionine gamma-lyase	CGL	↓	0.27	0.25	0.41	-	Tumor cells [61]	No	No
Q08257	Quinone oxidoreductase	QOR	↓	0.37	0.27	0.34	-	No	No	No
P60709	Actin, cytoplasmic 1	ACTB	↓	0.49	0.32	0.44	-	No	Yes	No
Q9Y696	Chloride intracellular channel protein 4	CLIC4	↓	0.33	0.25	0.41	-	No	Yes	No
Q96N87	Sodium-dependent neutral amino acid transporter B (0) AT3	S6A18	↓	0.08	0.09	0.16	-	No	No	No
P09211	Glutathione S-transferase P	GSTP1	↓	0.37	0.22	0.28	-	Tissue [37]	Yes	Yes
P48506	Glutamate--cysteine ligase catalytic subunit	GSH1	↓	0.48	0.31	0.41	-	Yes	No	No
O00338	Sulfotransferase 1C2A	S1C2A	↓	0.36	0.28	0.39	-	No	No	No
Q9UHI7	Solute carrier family 23 member1	S23A1	↓	0.25	0.18	0.20	-	No	Yes	No
P08236	Beta-glucuronidase	BGLR	↓	0.11	0.08	0.13	-	Tissue [62]	Yes	No
P23526	Adenosylhomocysteinase	SAHH	↓	0.25	0.23	0.33	-	No	No	No
O00299	Chloride intracellular channel protein 1	CLIC1	↓	0.45	0.34	0.49	-	Tissue [36]	Yes	No
O14745	Na (+)/ H (+) exchange regulatory cofactor	NHRF1	↓	0.38	0.28	0.37	-	No	Yes	No
Q9UNQ0	ATP-binding cassette	ABCG2	↓	0.32	0.27	0.41	-	No	Yes	No

	sub-family G member 2									
P08473	Neprilysin	NEP	↓	-	0.30	0.43	0.46	Tissue [63]	Yes	Yes
Q8WZ79	Deoxyribonuclease-2-beta	DNS2B	↑	-	4.18	3.26	2.42	No	No	No
P09417	Dihydropteridine reductase	DHPR	↓	-	0.40	0.42	0.45	No	No	No
Q8N5Z0	mitochondrial Kynurenine/ alpha-aminoadipate aminotransferase,	AADAT	↓	-	0.26	0.39	0.45	No	No	No
Q03154	Aminoacylase-1A	ACY1A	↓	-	0.48	0.41	0.49	No	Yes	No
P05186	Alkaline phosphatase	PPBT	↓	0.23	-	0.33	0.37	Tissue [26]	Yes	Yes
Q5T2W1	Na (+)/ H (+) exchange regulatory cofactor	NHRF3	↓	0.31	0.25	-	0.35	No	No	No
Q07075	Glutamyl aminopeptidase	SLC31	↓	0.36	0.25	0.27	0.38	No	Yes	No
Q07837	Neutral and basic amino acid transport protein rBAT	S7A13	↓	0.15	0.18	0.25	0.43	No	No	No
Q8TCU3	Solute carrier family 7 member13	EHD1	↓	0.16	0.13	0.21	0.43	No	Yes	No
Q9H4M9	EH domain-containing protein 1	SLC31	↓	0.13	0.19	0.27	0.46	No	Yes	No